comparable but slightly weaker hydrogen bonding near the protein surface.[2] Similar conclusions are drawn from IR measurements. It has also been deduced that the binding of water directly onto the surface of poly[2-(2-hydroxyethoxy)ethyl methacrylate] is not much stronger than the average mutual interaction between water molecules in the bulk.[11] A lack of information on the precise contribution of plasticized polymer to the type B signal precludes quantification of the number of water molecules per NVP or MMA unit.

In conclusion, comparison of DSC and NMR data provides interesting insight into the role of water in a range of hydrated P(NVP/MMA) samples. Three types of water are detected: tightly bound (type B), more loosely bound (type A), and bulk water. Both type A and type B water are nonfreezable in the accepted sense of the term but undergo glasslike transitions at 170–200 K. NMR is sensitive to both type A and type B water whereas DSC is sensitive only to type A. A scheme drawn up in terms of five thermodynamic equilibrium states facilitates the intercomparison of NMR and DSC data and clarifies the hysteresis effects observed in hydrated P(NVP/MMA).

Acknowledgment. It is a pleasure to acknowledge useful discussions with research personnel at Bausch and Lomb in Rochester, NY, and in Waterford, Ireland. This research was supported jointly by Bausch and Lomb and the Industrial Development Authority of Ireland.

Registry No. Lidofilcon, 56551-60-1; water, 7732-18-5.

References and Notes

(1) Rowland, S. P., Ed. *Water in Polymers*; ACS Symposium Series 127; American Chemical Society: Washington, DC, 1980.
(2) Kuntz, I. D.; Kauzmann, W. *Adv. Protein Chem.* **1974**, *28*, 239.
(3) McBrierty, V. I.; Douglass, D. C. *Phys. Rep.* **1980**, *63*, 61.
(4) Stillinger, F. H. In Reference 1, p 11.
(5) McCall, D. W. *NBS Spec. Publ. (U.S.)* **1969**, *No. 331*, 475. See also: Rowland, S. P.; Kuntz, I. L. In Reference 1, p 1.
(6) Puffr, R.; Sebenda, J. J. *Polym. Sci., Part C* **1967**, *16*, 79.
(7) Hatekeyama, T.; Yoshida, H.; Hatakeyama, H. *Polymer* **1987**, *28*, 1282.
(8) Moy, P.; Karasz, E. E. *Polym. Eng. Sci.* **1980**, *20*, 4.
(9) Jelinski, L. W.; Dumais, J. J.; Stark, R. E.; Ellis, T. S.; Karasz, F. E. *Macromolecules* **1983**, *16*, 1021.
(10) Pineri, M., Eisenberg, A., Eds. *Structure and Properties of Ionomers*; NATO ASI Series C; Reidel: 1987; Vol. 198.
(11) Pouchly, J.; Biros, J.; Benes, S. *Makromol. Chem.* **1979**, *180*, 745.
(12) Haly, A. R.; Snaith, J. W. *Biopolymers* **1971**, *10*, 1681.
(13) Rupley, J. A.; Yang, P.-H.; Tollin, G. In Reference 1, p 111.
(14) Boyle, N. G.; Coey, J. M. D.; McBrierty, V. J. *Chem. Phys. Lett.* **1982**, *86*, 3726.
(15) McBrierty, V. J.; Smyth, G.; Douglass, D. C. In Reference 10, p 149.
(16) Carr, H. W.; Purcell, E. M. *Phys. Rev.* **1954**, *94*, 630. Meiboom, S.; Gill, D. *Rev. Sci. Instrum.* **1958**, *29*, 688.
(17) Hartmann, S. R.; Hahn, E. L. *Phys. Rev.* **1962**, *128*, 2042.
(18) Powles, J. G.; Mansfield, P. *Phys. Lett.* **1962**, *2*, 58.
(19) McBrierty, V. J. *Polymer* **1974**, *15*, 503.
(20) Ratner, B. D.; Miller, I. F. *J. Polym. Sci., Polym. Chem. Ed.* **1972**, *10*, 2425.
(21) Douglass, D. C.; McBrierty, V. J. *Macromolecules* **1978**, *11*, 766.
(22) Albert, B.; Jerome, R.; Teyssie, P.; Smyth, G.; Boyle, N. G.; McBrierty, V. J. *Macromolecules* **1985**, *18*, 388.
(23) McBrierty, V. J.; Douglass, D. C. *Macromol. Rev.* **1981**, *16*, 295.
(24) Edzes, H. T.; Samulski, E. T. *Magn. Reson.* **1978**, *31*, 207.
(25) Chang, D. C.; Woessner, D. E. *Science (Washington, D.C.)* **1977**, *198*, 1180.
(26) Resing, H. A.; Foster, K. R.; Garroway, A. N. *Science (Washington, D.C.)* **1977**, *198*, 1181.
(27) Zimmerman, J. R.; Brittin, W. E. *J. Phys. Chem.* **1957**, *61*, 1328.
(28) Resing, H. A. *Adv. Mol. Relax. Processes* **1972**, *3*, 199.
(29) Hoeve, C. A. J. In Reference 1, p 135.
(30) Boyle, N. G.; McBrierty, V. J.; Douglass, D. C. *Macromolecules* **1983**, *16*, 75.
(31) See, for example: Wong, T. C.; Ang, T. T. *J. Phys. Chem.* **1985**, *89*, 4047.
(32) Wardell, G. E.; McBrierty, V. J. *Proc. R. Ir. Acad., Sect. A* **1973**, *73*, 63.
(33) Ladbrooke, B. D.; Jenkinson, T. J.; Kamat, V. B.; Chapman, D. *Biochim. Biophys. Acta* **1968**, *164*, 101.
(34) Lee, H. B.; Jhon, M. S.; Andrade, J. D. *J. Colloid Interface Sci.* **1975**, *51*, 225.
(35) Katayama, S.; Fujiwara, S. *J. Phys. Chem.* **1980**, *84*, 2320.
(36) The units calories per gram have been retained to facilitate comparison with the significant body of comparable data in the literature.

Water in Hydrogels. 2. A Study of Water in Poly(hydroxyethyl methacrylate)

Gerard Smyth, Francis X. Quinn, and Vincent J. McBrierty*

Department of Pure and Applied Physics, Trinity College, Dublin 2, Ireland.
Received January 21, 1988; Revised Manuscript Received April 27, 1988

ABSTRACT: Collated broad-line NMR and DSC measurements sensitively probe the behavior of water in hydrated poly(hydroxyethyl methacrylate) (PHEMA). NMR reveals that bound water becomes mobile at ~180 K in keeping with observations in many other hydrated polymers; DSC is insensitive to events at these temperatures. In samples with a high water content, a fraction of this mobile water subsequently freezes between 230 and 260 K. The amount of freezable and nonfreezable water in hydrated PHEMA is determined quantitatively. Preliminary cross-relaxation experiments at 253 and 293 K indicate that NMR spin–lattice relaxation rates for water will be overestimated if the effects of cross-relaxation between the polymer and water proton spin systems are neglected. Although PHEMA is less hydrophilic than poly(*N*-vinyl-2-pyrrolidone/methyl methacrylate), studied in part 1, the *relative* fraction of bound water is significantly higher. Hysteresis effects in hydrated PHEMA are investigated in some detail.

Introduction

Part 1 of this study,[1] the preceding paper in this issue, briefly reviewed the general literature on hydrogels and examined specifically the role of water in poly (*N*-vinyl-2-pyrrolidone/methyl methacrylate) copolymer P(NVP/MMA). This paper reports on a second hydrogel, poly(hydroxyethyl methacrylate) (PHEMA), whose properties differ in a number of intriguing ways from those of P(NVP/MMA).

PHEMA has received wide attention primarily due to its biological compatibility.[2-14] Swelling experiments[10] indicate a secondary noncovalent structure superimposed

0024-9297/88/2221-3198$01.50/0

on the principal covalently bonded cross-linked network. It has been attributed to hydrophobic interactions between α-methyl groups and/or chain backbones,[5] hydrogen-bonded hydroxyl groups,[10] or interactions involving both hydroxyl and carboxyl groups.[14]

In experiments where water is incorporated at the polymerization stage and the concentrations reported are relative to the hydrated polymer, gels are homogeneous and clear for water contents up to 40 wt % and are heterogeneous and visually turbid[5,7-9,11] at higher levels of hydration. Three types of water have been proposed in hydrated PHEMA: bound water (≤20 wt %) corresponding to an average of two water molecules hydrogen-bonded to each repeat unit;[11,15] interfacial water, attributed to dipole–dipole interactions with hydroxyl groups[14] or hydrophobic interactions with polymer segments,[16] and freely diffusable water in samples where the level of hydration exceeds 35 wt %. The fraction of each type of water is influenced by the degree of cross-linking,[14] and hysteresis effects are observed.[11] An ability to distinguish between different types of water in hydrogels facilitates understanding of their transport properties.[12]

In keeping with the general approach enunciated in part 1, coordinated NMR and DSC experiments lead to a clearer understanding of the role water in PHEMA. In addition, a comparison of results for PHEMA and P(NVP/MMA) reveals characteristic subtleties in the way in which water behaves in each system and cautions against overgeneralization.

Experimental Section

The experimental procedures used in the acquisition and analysis of NMR and DSC data are discussed fully in part 1.[1] Briefly, proton spin–spin (T_2), spin–lattice (T_1), and rotating frame ($T_{1\rho}$) relaxation times were recorded on a Bruker SXP spectrometer operating at 40 MHz. More sophisticated pulse sequences to probe specific aspects of water behavior are alluded to in later discussion. DSC thermograms were recorded on a Perkin-Elmer DSC-4 differential scanning calorimeter interfaced to a thermal analysis data System.

The PHEMA material, available commercially as Polymacon, contained trace amounts of ethylene glycol dimethacrylate (0.4 wt %) and benzoin methyl ether (0.2 wt %). Hydration procedures and nomenclature are as reported in part 1:[1] samples designated S(W) contain W wt % water relative to the 100 wt % dry polymer, S(0). In this study, water is incorporated after polymerization. Unless otherwise specified, all data were recorded as a function of increasing temperature after quenching the sample in liquid nitrogen.

Results and Discussion

NMR Results. Proton T_1, T_2, and $T_{1\rho}$ vs temperature for the dry polymer S(0) are presented in Figure 1. Again α-methyl group motion dominates T_1 and $T_{1\rho}$ relaxation at ~280 and ~200 K, respectively. It is interesting that the T_1 minimum at 150 K in poly(ethyl methacrylate) (PEMA) is absent in PHEMA confirming the earlier assignment of this relaxation in PEMA to motions involving side-chain methyl groups.[17]

NMR data for the water-saturated polymer S(53) are portrayed in Figure 2. Note that PHEMA can support much less water than P(NVP/MMA). The T_1 minimum at 225 K, the lower of the two $T_{1\rho}$ minima at ~200 K, and the onset of the long, T_{2L}, component at about 180 K are characteristic of glasslike water. The shoulder in T_1 at ~280 K and the longer minimum in $T_{1\rho}$ at 200 K denote α-CH_3 relaxation. The fact that the magnitude of this $T_{1\rho L}$ minimum is less than half its magnitude in the dry polymer implies that relaxation associated with the water glass transition and the α-CH_3 motion are coupled.[18] The hysteresis in T_{2L} and T_1, the nonexponential decay in $T_{1\rho}$,

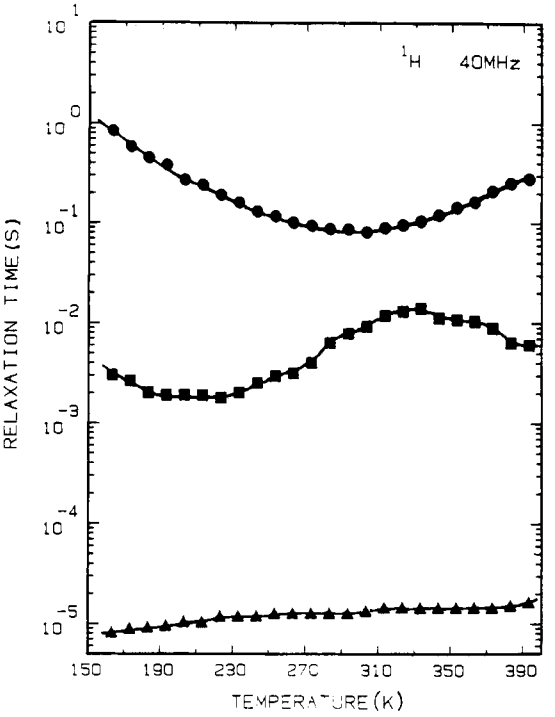

Figure 1. Proton T_1 (●), $T_{1\rho}$ (■) (H_1 = 10G), and T_2 (▲) results for dry PHEMA, S(0), as a function of temperature.

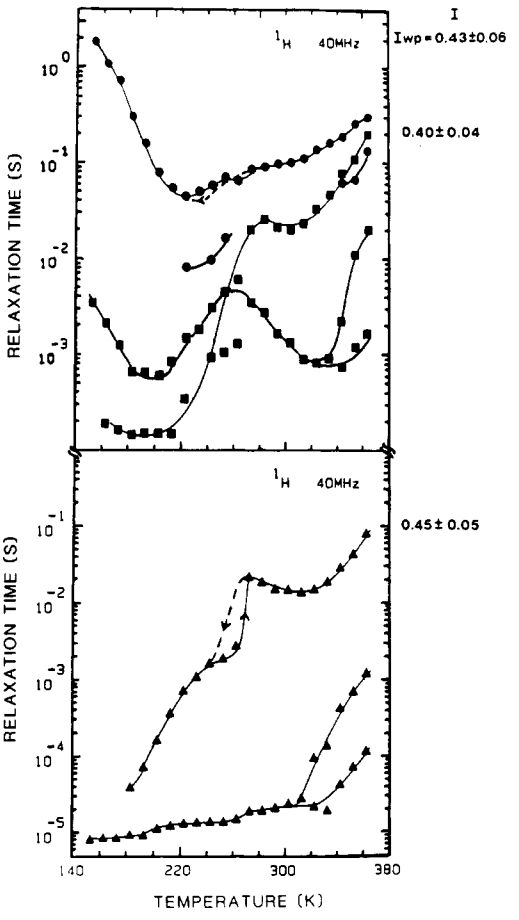

Figure 2. Proton T_1 (●), $T_{1\rho}$ (■) (H_1 = 10G), and T_2 (▲) for saturated PHEMA, S(53), as a function of temperature. The dashed curves denote the decreasing temperature cycle. $T_{1\rho L}$ and T_{2L} component intensities in the high-temperature region are as indicated on the left-hand side of the diagram. I_{WP} is the calculated water proton intensity (see Table I).

and the increase in the short, T_{2S}, component by about a factor of 2 between 240 and 280 K are all characteristic

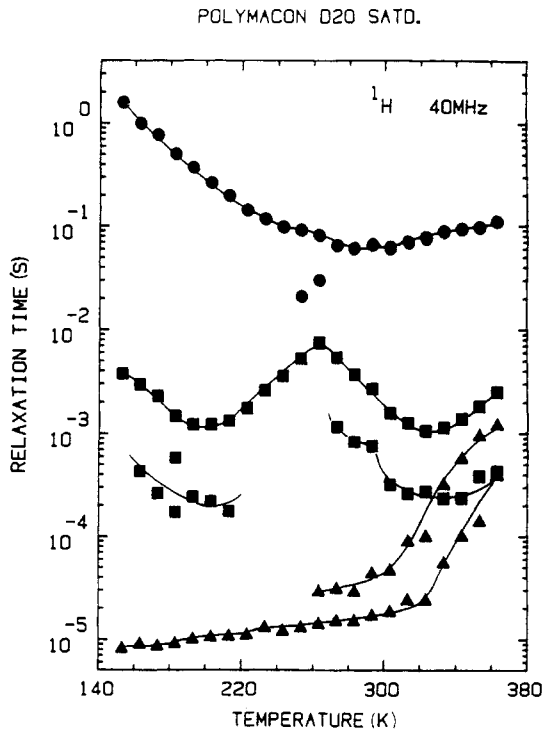

Figure 3. Proton T_1 (●), $T_{1\rho}$ (■) (H_1 = 10G), and T_2 (▲) for PHEMA saturated with D_2O as a function of temperature.

of complex behavior as was observed in P(NVP/MMA) in this temperature range. The increase in T_{2S} and 260 K is the first manifestation of plasticization, leading ultimately to a premature onset of general motions in saturated PHEMA relative to the dry polymer (Figure 1). The temperature dependence of T_{2S} and T_{2i} above room temperature is reminiscent of selective plasticization in PVC.[19] Assignment of T_{2L} to water behavior is dictated by the excellent agreement between the computed fraction of water protons and the intensity of T_{2L} (and $T_{1\rho L}$) in the high-temperature regime (Figure 2). The broad T_{2L} minimum above room temperature is in accord with Resing's predictions for chemical exchange between different water sites in the polymer[20] and represents an average over a heterogeneous distribution of water environments above 273 K.

Proton data for PHEMA saturated with D_2O (Figure 3) confirm these general perceptions. NMR features associated with a glasslike water response are largely absent, but the short $T_{1\rho S}$ component ($I \approx 0.15$) at ~200 K may well be due to residual water in the sample. The onset of T_{2L} at ~260 K, the subsequent increase in T_{2S}, at ≃320 K, the corresponding $T_{1\rho}$ minima at about 325 and 335 K, and the observation that T_1 is generally shorter than T_1 for S(0) above room temperature are all manifestations of extensive polymer plasticization. The dominant low-temperature $T_{1\rho}$ minimum ($I \approx 0.85$) and the modest increase in T_2 at ~200 K reflect α-CH_3 group relaxation.

More sophisticated NMR experiments can be deployed to probe further the way in which water behaves in PHEMA. Consider, for example, the Goldman–Shen pulse sequence (Figure 4a) used in earlier studies to monitor spin diffusion in solid polymers[21] and cross-relaxation between different phases in hydrated collagen and elastin.[22] In a composite system characterized by short and long T_2 relaxation times, the choice of τ_1 which satisfies the condition $T_{2S} \ll \tau_1 \ll T_{2L}$ randomizes the proton spins associated with T_{2S} without unduly perturbing the phase coherence of the more mobile spins. The magnetization remaining after τ_1 is realigned along the laboratory magnetic field by

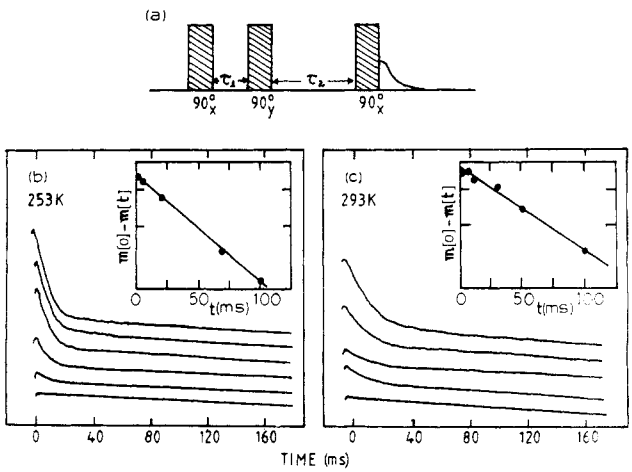

Figure 4. (a) Goldman–Shen pulse sequence. (b) Free induction decays for saturated PHEMA at 253 K, where τ_1 = 70 μs and, proceeding vertically, τ_2 = 0.1, 5, 20, 70, 100, and 500 ms. (c) Free induction decays for saturated PHEMA at 293 K where τ_1 = 70 μs and, proceeding vertically, τ_2 = 0.1, 5, 8, 50, and 500 ms. Successive traces in a and b are displaced vertically for clarity of presentation.

using the 90°$_y$ pulse where subsequent transfer of spin energy to the more mobile component via cross-relaxation is monitored at subsequent times τ_2 with the third, 90°$_x$, pulse. Typical results for saturated PHEMA at 253 and 293 K are presented in parts b and c of Figure 4, respectively. When insufficient time (short τ_2) is allowed for cross-relaxation to equilibrate the two phases, only the long T_2 decay is observed. At longer τ_2 the change in the shape of the decay, due to the reappearance of the short T_2 component, without significant increase in the initial intensity of the FID, signifies a transfer of spin energy from the short to the long T_2 component. Inspection of the two sets of data reveals that the cross-relaxation process is first detected on a time scale of few milliseconds, which is in keeping with similar observations in hydrated elastin.[22] For much longer τ_2, the return to equilibrium is governed by T_1 as shown in the inserted plots of $M(\infty) - M(\tau_2)$ vs τ_2, from which T_1(253K) = 70 ms and T_1(293K) = 110 ms, in agreement with the T_1 results in Figure 2.

A second experiment devised by Edzes and Samulski[18] has been exploited to great effect in monitoring cross-relaxation in hydrated collagen. In their "selective hydration inversion technique", the length of the 180° pulse, τ_{180}, in the 180°–τ–90° sequence usually employed to measure T_1 is manipulated to achieve full inversion of the water proton magnetization and partial inversion of the macromolecular magnetization. This occurs when $T_{2\text{macro}} < \tau_{180} \ll T_{2\text{water}}$. Typical data at 293 K showing the change in the magnetization decay of the water and macromolecular protons in saturated PHEMA as a function of τ_{180} (Figure 5) can be analyzed to give a number of important relaxation parameters by using the following expressions:[18]

$$m_i(t) = C_i^+ \exp(-R_1^+ t) + C_i^- \exp(-R_1^- t) \quad (1)$$

$$2R_1^{\pm} = R_{1i} + R_{1j} + k_i + k_j \pm [(R_{1i} - R_{1j} + k_i + k_j)^2 + 4k_i k_j]^{1/2} \quad (2)$$

$$C_i^{\pm} = (R_1^+ - R_1^-)^{-1} \pm [m_i(0)(R_{1i} - R_1^{\pm}) \pm (m_i(0) - m_j(0))k_i] \quad (3)$$

$$p_i k_i = p_j k_j \quad (4)$$

$R_1^{\pm}$ and $C_i^{\pm}$ are the observed relaxation rates and component intensities (Figure 5), R_i is the spin–lattice relaxation rate of the i phase in the absence of cross-relaxation,

Table I
Pertinent T_2 Intensity Data for PHEMA (Figure 7)

sample	I_{WP}[a]	experimental intensities			relative fraction of each component[b]	
		I_{L1}	I_{L2}	I_{L4}	I_{L1}/I_{WP}	I_{L2}/I_{WP}
S(53)	0.43	0.42	0.33	0.48	0.98 (52)	0.77 (41)
S(46)	0.40	0.35	0.32	0.46	0.88 (40)	0.80 (37)
S(20)	0.23	0.24	0.22	0.22	1.0 (20)	1.0 (20)
S(9)	0.11	0.12	0.12	0.12	1.0 (9)	1.0 (9)

[a] Fraction of water protons. [b] The numbers in parentheses denote the corresponding weight percentages relative to the dry polymer. The error in the relative fraction of each component is of the order of 15%.

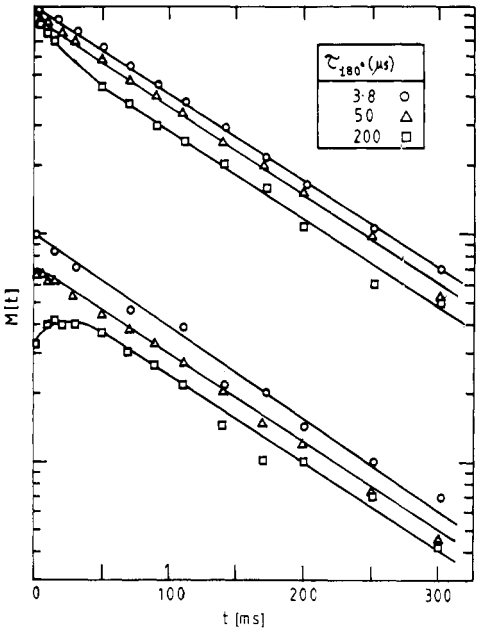

Figure 5. Effect of the 180° pulse length, $\tau_{180}°$, on the proton spin–lattice decay for the water magnetization $m_w(t)$ (upper curves) and the macromolecular magnetization $m_m(t)$ (lower curves) in PHEMA. The data are fitted to eq 1 by using the parameters given in the text. Method II of Edzes and Samulski's paper[18] was used to record these data.

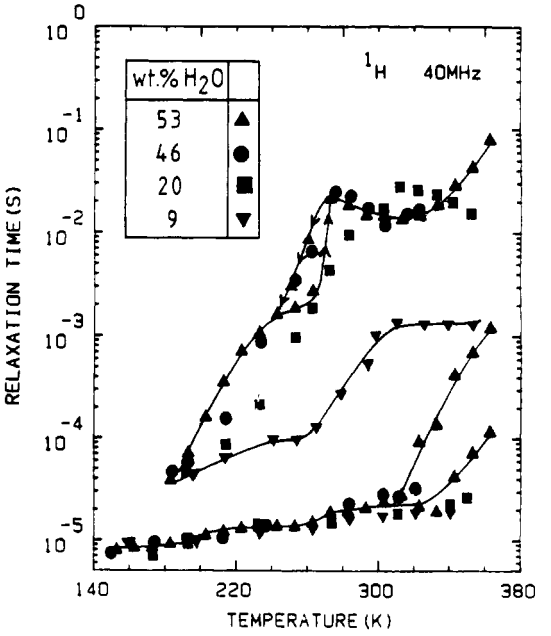

Figure 6. Proton T_2 for hydrated PHEMA as a function of temperature and water content.

k_i is the rate of transfer of magnetization out of the i phase, and p_i is the fraction of protons in the i phase. Fitting eq 1 to the experimental data in Figure 5 provides $R_1^- = 9.0 \pm 0.9\ s^{-1}$ and $R_1^+ = 65 \pm 7\ s^{-1}$. As reported later in Table I, $p_m = 0.57 \pm 0.06$ and $p_w = 0.43 \pm 0.06$. The results for PHEMA saturated with D_2O (Figure 3) indicate that $R_{1m} = T_{1m}^{-1} = 17 \pm 2\ s^{-1}$ at 293 K. With this information, the following additional parameters are determined from eq 2–4: $R_{1w} = 7 \pm 2\ s^{-1}$, $k_w = 22 \pm 6\ s^{-1}$, and $k_m = 16 \pm 7\ s^{-1}$.

An important conclusion of this experiment is that the true water spin–lattice relaxation rate R_{1w} is overestimated by about 29% if it is equated to the measured rate R_1^- as would be the case if cross-relaxation effects were neglected. A more comprehensive analysis of cross-relaxation in hydrated PHEMA is contemplated in a later publication.

Figure 6 describes the dependence of T_2 on water content. T_{2S} is essentially invariant to the degree of hydration below the transition beginning at ~260 K after which plasticization is evident in samples of higher water content, culminating in the premature onset of general polymeric motions above ~310 K. Mobility in the glasslike water, as reflected in T_{2L}, sets in at a marginally lower temperatures in the more heavily hydrated samples, and the way in which T_{2L} increases subsequently with temperature depends on the level of hydration. At low water concentrations the slow and nonuniform increase in T_{2L} reflects a broad distribution of correlation times typical of motions that are, on average, much more constrained than in samples of PHEMA with higher water contents. As with P(NVP/MMA), there is no dramatic change in T_2 as 273 K is approached although appreciable hysteresis in T_{2L} is observed in S(53). This hysteresis is particularly significant and will be explored further at a later point in the discussion.

The minimum in T_{2L} associated with chemical exchange is centered at ~310 K in S(53) and S(46), and there are the first signs of a similar minimum at a higher temperature in S(20). (Data were not recorded at higher temperatures to avoid loss of water from the hydrated polymer.) The magnitude of T_{2L} above room temperature in the fully hydrated sample S(53) representing water averaged over all environments is significantly less than T_{2L} for saturated P(NVP/MMA) but of comparable magnitude in P(NVP/MMA) samples of *similar* water content. This implies that water is less bulklike and more tightly associated or bound in saturated PHEMA. Whereas PHEMA is less hydrophilic than P(NVP/MMA), the *relative* amount of water that is tightly bound in fully hydrated PHEMA is very much higher than in saturated P(NVP/MMA). These differences in affinity for water arise from factors intrinsic to the polymer and also from experimentally controlled parameters such as the degree of cross-linking, as alluded to in Part 1.[1]

T_2 component intensity data presented in Figure 7 display the following features and in some respects differ from the results for hydrated P(NVP/MMA): (*i*) Mobility sets in at 170 K and, ultimately, I_L attains a value that is in reasonable agreement with the calculated water proton fraction. (*ii*) A minimum in I_L vs temperature is observed

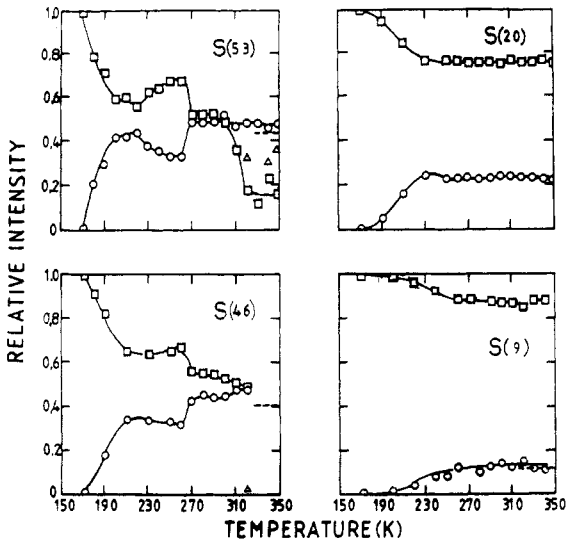

Figure 7. T_2 component intensity data as a function of temperature and water content: I_L (○), I_i (△), I_s (□). The dashed lines denote the calculated fraction of water protons.

at ~250 K in S(53) and S(46), but, in contrast to P(NVP/MMA), the loss of intensity from I_L is reflected in a proportionate increase in I_S rather than in the creation of a second, somewhat less mobile water plus plasticized polymer component. These observations are consistent with the formation of ice as the temperature is increased from 230 to 260 K, a process that has been termed *devitrification*.[23] (*iii*) The modest extent to which I_L increases in the vicinity of 273 K, even in saturated material, further confirms that the amount of bulklike water in PHEMA is small.

Following the nomenclature and procedures used in part 1, the maximum intensity of the mobile T_2 component below 273 K is denoted I_{L1}, the intensity at the minimum near 260 K is I_{L2}, and I_{L4} is the magnitude of I_L in the high-temperature regime. The relevant data in Table I confirm that the bulk of the water in hydrated PHEMA is rendered mobile at low temperatures, characteristic of bound water. Between 240 and 260 K, however, some 10% of the mobile water in S(53) and ~3% in S(46) freezes again. The significance of these results will be discussed later when the DSC data are considered.

Reverting to the T_{2L} hysteresis in S(53), Figure 8 presents data for a number of sequential thermal cycles on a freshly prepared saturated sample, S(56). The original results for S(53) (Figures 3 and 5) are represented by the dashed lines in Figure 8.

Cycle A. The sample is quenched from room temperature (open circles) to the desired temperature under free cooling conditions.

Cycle B. After quenching in liquid nitrogen from room temperature, the sample is heated in steps to room temperature (open triangles), and, as before, a shoulder in T_{2L} is observed. I_L forms a minimum at 263 K, in keeping with earlier observations on S(53).

Cycle C. In this final temperature cycle, the sample is first quenched in liquid nitrogen, subsequently annealed at 263 K for 30 min, and then progressively cooled in the spectrometer to give the data denoted by the open squares.

On cooling from room temperature under cycle A, T_{2L} remains long and the minimun in I_L is shallow, in accord with the notion that no more than a modest amount of ice is formed. In cycle B, ice which is generated upon quenching in liquid N_2 acts as a nucleating agent for the formation of more ice between 210 and 270 K. The appreciable mobility of bound water in this temperature

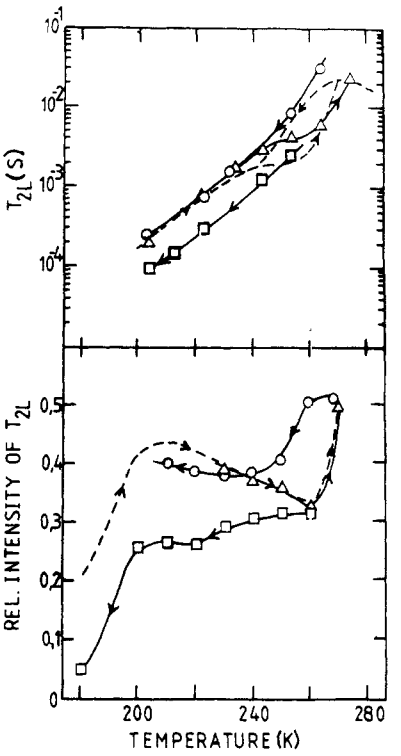

Figure 8. Effect of thermal cycling on T_{2L} and I_L in hydrated PHEMA, S(56) (see text).

range facilitates contact between the nucleating centers and mobile water. However, the fact that only part of the mobile water participates in the devitrification process supports the concept of a heterogeneous distribution of water sites with differing barriers to translational diffusion as proposed in Resing's model for water adsorbed in porous media.[20] The shoulder in T_{2L} and the much deeper minimum in I_L reflect a reduced contribution of the more mobile water to T_{2L}, thus biasing the relaxation time toward longer correlation times and a shorter T_{2L}. Annealing the sample at 263 K (cycle C) maximizes the formation of ice from the mobile bound water phase, and once ice is formed at 263 K it does not melt again on subsequent cooling, as shown clearly in the intensity response (open squares).

DSC Results. Representative endothermic peaks for PHEMA are presented as a function of water content in Figure 9. Unlike hydrated P(NVP/MMA), a sensitivity to scan rate was observed; peaks recorded at 5 K min^{-1} developed structure, and the associated heats of fusion were higher. This is shown rather vividly in Figure 10 for sample S(40) subjected to successive heating and cooling cycles of 20 and 5 K min^{-1}, respectively. The data for S(49) in the insert of Figure 9 are typical of heavily hydrated PHEMA in the way that a broad rather shallow exothermic trough between ~230 and 260 K precedes the formation of the sharp endotherm associated with the thawing of frozen water during the heating cycle. This supports the earlier conclusion that ice is formed.

Collated endothermic results for PHEMA presented in Figure 11 show the integrated change in enthalpy as a function of water content. Data recorded at 20 and 5 K min^{-1} respectively predict 27 ± 4 and 25 ± 4 wt % as the maximum amount of nonfreezable water in PHEMA. These values agree within experimental error. The differential heats of fusion, ΔH_f, for the higher and lower scanning rates are 17 ± 4 and 23 ± 7 cal g^{-1}, respectively. One sample, S(52), which contained an unusually high amount of water for PHEMA exhibited what appeared to

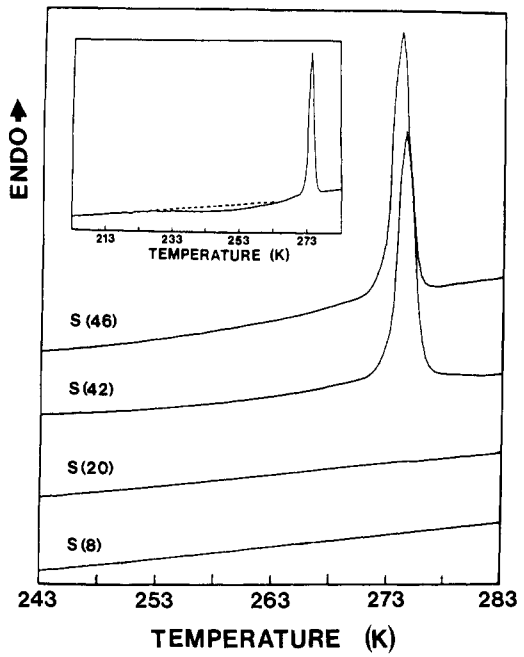

Figure 9. DSC endothermic peaks for a range of hydrated PHEMA samples. Scan rate = 20 K min^{-1}. Note the shallow exotherm between 223 and 263 K; it is most clearly evident in S(49), as shown in the insert.

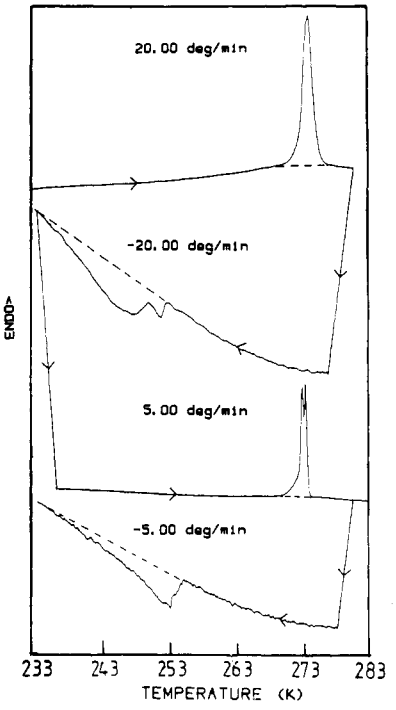

Figure 10. Effect of thermal cycling and scan rate on the DSC response for PHEMA sample S(40).

be an anomalously high value for ΔH_f, more characteristic of bulklike water. It is interesting to note that data recorded at the lower scan rate extrapolate to a comparably high ΔH_f, indicating that differences in scan rate become less important for water which is more bulklike, as was the case for hydrated P(NVP/MMA).

The broad exothermic troughs generated in the cooling cycles fall within the temperature range 230–255 K and reflect small changes in enthalpy (Figure 10). The corresponding heat of fusion is $\Delta H_f = 6 \pm 2$ cal g^{-1}, and, in contrast to hydrated P(NVP/MMA), the maximum amount of nonfreezable water predicted in the heating and cooling cycles is of comparable magnitude, 25 ± 3 wt %.

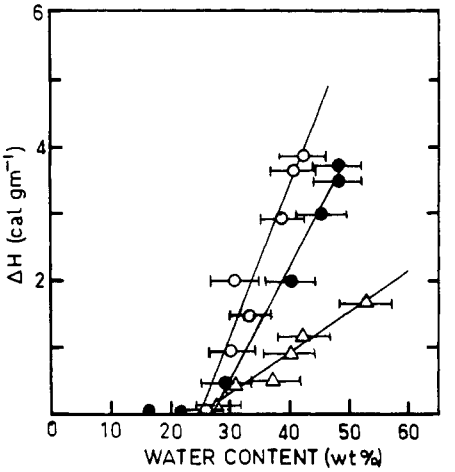

Figure 11. Plot of ΔH vs water content for endothermic peaks at 20 K min^{-1} (●), 5 K min^{-1} (○), and exothermic troughs (△). Regression fits to the data are as follows: (●) $\Delta H = 0.17W - 4.54$ ($R = 1.00$), (○) $\Delta H = 0.23W - 5.67$ ($R = 0.97$), (△) $\Delta H = 0.06W - 1.49$ ($R = 0.98$). Both ΔH and water content are relative to the dry polymer weight.

As in earlier measurments, DSC is insensitive to events below 230 K where NMR reveals a much higher fraction of water that becomes mobile at ~180 K. This insensitivity does not imply that freezing or thawing is not taking place, merely that the associated change in heat capacity is too small to be detected by DSC. The glasslike water is characteristically heterogeneous and again departs from P(NVP/MMA) behavior in the way that part of the mobile bound component subsequently freezes or devitrifies during the heating cycle. The DSC estimate of the nonfreezable fraction (25 ± 4 wt %) is lower than that predicted by NMR (39 ± 6 wt %) at comparable temperatures. This is not particularly surprising since T_{2L} in this case includes contributions designated type B in part 1 to which DSC is insensitive.

In summary, collated NMR and DSC data provide useful insight into the way in which water behaves in hydrated PHEMA. Bound water which becomes mobile at ~180 K displays the characteristics of a glass in common with many other hydrated polymer systems.[1] A fraction of this low-temperature mobile component subsequently freezes. Water behavior is predictably complex in the vicinity of 273 K, and chemical exchange effects are readily apparent in T_{2L} data above room temperature. Preliminary cross-relaxation experiments indicate that the spin–lattice relaxation rate for water will be overestimated by about 29% if the effects of cross-relaxation are neglected. Although PHEMA is less hydrophilic than P(NVP/MMA), the relative proportion of bound water is higher. Significant hysteresis effects are observed in the saturated sample.

Acknowledgment. This work forms part of an ongoing research program sponsored jointly by Bausch and Lomb (Rochester, NY, and Waterford, Ireland) and the Industrial Development Authority of Ireland.

Registry No. PHEMA, 25053-81-0; water, 7732-18-5.

References and Notes

(1) Quinn, F. X.; Kampff, E.; Smyth, G.; McBrierty, V. J.
(2) Rowland, S. P., Ed, *Water in Polymers*; ACS Symposium Series 127; American Chemical Society: Washington, DC, 1980.
(3) Refojo, M. F.; Yasuda, H. J. *J. Appl. Polym. Sci.* **1965**, *9*, 2425.
(4) Yasuda, H.; Gochin, M.; Stone, W. Jr. *J. Polymn. Sci., Polym. Chem. Ed.* **1966**, *4*, 2913.
(5) Refojo, M. F. *J. Polym. Sci., Polym. Chem. Ed.* **1967**, *5*, 3103.
(6) Baresova, V. *Collect. Czech. Chem. Commun.* **1969**, *34*, 707.

(7) Ilavsky, M.; Prins, W. *Macromolecules* **1970**, *3*, 415.
(8) Gouda, J. H.; Provodator, K.; Warren, T. C.; Prins, W. J. *Polym. Sci., Part B* **1970**, *8*, 225.
(9) Dusek, K.; Sedlacek, B. *Eur. Polym. J.* **1971**, *7*, 1275.
(10) Ratner, B. D.; Miller, I. F. *J. Polymn. Sci., Polym. Chem. Ed.* **1972**, *10*, 2425.
(11) Lee, H. B.; Jhon, M. S.; Andrade, J. D. *J. Colloid Interface Sci.* **1975**, *51*, 225.
(12) Pedley, D. G.; Tighe, B. J., *Br. Polym. J.* **1979**, *11*, 130.
(13) Zentner, G. M.; Cardinal, J. R.; Kim, S. W. *J. Pharm. Sci.* **1978**, *67*, 1352.
(14) Collett, J. H.; Spillane, D. E. M.; Pywell, E. J. *Polym. Prepr. (Am. Chem. Soc., Div. Polym. Chem.)* **1987**, *28*, 141.
(15) Pedley, D. G.; Tighe, B. J. *Br. Polym. J.* **1979**, *11*, 130.
(16) Kim, S. W.; Cardinal, J. R.; Wisniewski, S.; Zentner, G. M. In Reference 2, p 347.
(17) Douglass, D. C.; McBrierty, V. J. *Macromolecules* **1978**, *11*, 766.
(18) Edzes, H. T.; Samulski, E. T. *J. Magn. Reson.* **1978**, *31*, 207.
(19) Douglass, D. C. *ACS Symp. Ser.* **1980**, *No. 142*, 147. See also: McBrierty, V. J. *Faraday Discuss. R. Soc. Chem.* **1979**, *68*, 78.
(20) Resing, H. A. *Adv. Mol. Relax. Processes* **1972**, *3*, 199.
(21) McBrierty, V. J.; Douglass, D. C. *Phys. Rep.* **1980**, *63*, 61.
(22) Wise, W. B.; Pfeffer, P. E. *Macromolecules* **1987**, *20*, 1550.
(23) Murase, N.; Gonda, K.; Watanabe, T. *J. Phys. Chem.* **1986**, *90*, 5420.

The Flory χ Parameter and Phase Separation in Semidilute Polymer Mixtures: A Renormalization Group Study

Binny J. Cherayil† and Karl F. Freed*

The James Franck Institute and the Department of Chemistry, The University of Chicago, Chicago, Illinois 60637. *Received October 20, 1987; Revised Manuscript Received April 22, 1988*

ABSTRACT: The universal part of the free energy of mixing of semidilute solutions of two polymers in marginal to good solvents is evaluated by using an Edwards' continuum model. Excluded-volume interactions between chains are modeled by the usual δ function pseudopotentials, while polymer–solvent interactions are introduced via the Flory–Huggins lattice theory by requiring that the lattice and continuum theory free energies of mixing coincide at the Θ point. The free energy is calculated perturbatively near four dimensions ($d = 4$) as an expansion to first order in $4 - d$. A renormalized free energy is defined through the introduction of phenomenological osmotic second virial coefficients that absorb divergences in the perturbation expansion. By deriving expressions for the chemical potentials of the various components of the ternary mixture, the Flory χ parameters are obtained as functions of concentration, molecular weight, and temperature. They cannot be represented as pairwise additive polymer–solvent and polymer–polymer contributions because of the screening of excluded-volume interactions in semidilute solutions. Equations for the coexistence curves for phase separation are determined for two special limits, and the predictions are compared with the Flory–Huggins theory. A general theorem is proven that phenomenologically defined Flory χ parameters of ternary mixtures must diverge in the limit that the volume fraction of one of the components vanishes, provided certain regularity constraints are obeyed by the chemical potentials in this limit.

1. Introduction

The study of solutions or blends of different polymers is important in a number of areas of polymer processing, including the development of composites, biological fractionation, and colloid chemistry.[1-3] As a result, these systems have been the subject of numerous experimental[4] and theoretical[5] investigations.

Our present understanding of the salient entropic and enthalpic changes accompanying the formation of polymer mixtures relies heavily on the early lattice theory of mixing of Flory, Huggins, and others[6] for polymer blends. Blends are especially amenable to mean-field treatments of the Flory–Huggins kind as the composition fluctuations in these systems are small over a wide range of temperatures. However, Flory–Huggins-type approaches do not adequately describe the behavior of polymers in semidilute solutions, where long-range correlations lead to the emergence of altered power law dependences of effective interaction energies, osmotic pressures, etc., on concentration. Here we study the free energy of mixing of moderate to good solvent semidilute binary polymer mixtures using renormalization group methods to investigate the concentration dependence of the Flory χ parameter and to explore the ramifications of the abovementioned altered power-law dependences on the coexistence curve for phase separation.

The systematic description of polymers in semidilute solutions has recently been made possible by the methods of the renormalization group[7] (for a detailed discussion, see, for example, ref 8). But the application of these methods to the study of mixtures has so far been somewhat limited.[5d,e] For instance, there is presently no renormalization group treatment of demixing in the simplest system of a mixture of a polymer and a solvent. The difficulties of such a treatment are associated with the necessity of at least including both two- and three-body excluded-volume interactions in the theory.[9] No satisfactory way to do this is yet known for arbitrary values of the two interactions, i.e., away from the theta region. (But see ref 10 for a mean-field treatment.)

Renormalization group approaches are more readily applied to mixtures in which the effects of three-body interactions are unimportant. For example, Schäfer and Kappeler[5d] determine the renormalized spinodal for a ternary solution of two polymers in a solvent that is marginal to good for both polymers. Their calcualtion uses the "tree approxiamtion", however, and thereby neglects excluded-volume screening, which first appears only in the next order in excluded volume and which describes important effects of long-range correlations in semidilute polymer solutions. Although even the mean-field calculations of Schäfer and Kappeler produce qualitative departures from the standard Flory–Huggins theory, Schäfer and Kappeler note that a complete description of critical

† Present address: Baker Laboratory of Chemistry, Cornell University, Ithaca, NY 14853.

0024-9297/88/2221-3204$01.50/0